

# Indentation Deformation and Fracture of Sapphire

HELEN M. CHAN\* and BRIAN R. LAWN\*

Ceramics Division, Institute for Materials Science and Engineering, National Bureau of Standards, Gaithersburg, Maryland 20899

Relatively little is known about the fundamental deformation processes in intrinsically hard, brittle materials, and even less about how these processes lead to the initiation of cracks. In this paper, transmission electron microscopy is used to study the deformation structure within Vickers indentation zones of single-crystal sapphire with  $\{11\bar{2}0\}$  surface orientation. The relative misorientation of regions within these zones, as mapped by convergent-beam kikuchi patterns, is found to be severe, indicative of shear processes operating close to the cohesive limit. Two principal types of deformation are identified, basal twinning and pyramidal slip. Incipient microcracks are observed at both the twin interfaces and the slip planes. These incipient "flaws" act as nucleation sites for the ensuing radial and lateral cracks.

## I. Introduction

IN RECENT years, indentation analysis<sup>1-3</sup> has emerged as a powerful tool for evaluating and characterizing the deformation and fracture properties of ceramic materials, particularly as quantified by hardness and toughness.<sup>4-6</sup> The basic concept behind indentation testing is attractive in its simplicity. A standard "sharp" indenter (e.g., Vickers) is loaded onto the surface of the test material. The intense stress concentration beneath the indenter contact causes the material to undergo both reversible and irreversible deformation. The most obvious manifestation of the latter component is, of course, the residual hardness impression. The irreversible component is also responsible for any attendant crack initiation.<sup>7-10</sup> Furthermore, residual stresses can continue to exert a strong influence on crack propagation well beyond the near-contact zone.<sup>2,3,11,12</sup> A fundamental understanding of contact-induced deformation processes would therefore appear to be an essential prerequisite to any complete description of flaw micro-mechanics in highly brittle ceramics.

A notable restriction implicit in present-day indentation fracture mechanics is the assumption of homogeneity and isotropy of material structure. This restriction is apparent in experimental as well as theoretical work, particularly in the strong tendency to adopt silicate glasses as model test materials. Studies into the mechanisms of indentation-induced crack initiation have been carried out almost exclusively on glasses.<sup>7-10</sup> Such studies reveal the sources of initiation in the amorphous structures as "shear faults" punched in irreversibly by the penetrating indenter. Characteristic of these faults is that they form on curved surfaces, governed by trajectories of maximum shear, at stress levels close to the theoretical cohesive limit. Such characteristics would appear to represent a substantial departure from our traditional notions of slip deformation in crystalline materials by low-stress dislocation processes. Yet there are general features of the indentation deformation/fracture pattern in brittle materials, not least the clear tendency for the radial cracks to initiate near the impression corners, that suggest some commonality in underlying mechanisms. The implication here is that the classical picture of crystal plasticity by dislocation glide may require some qualification when applied to ceramics, especially to the tougher, harder ceramics with intrinsically strong covalent-ionic bonding.

Accordingly, the purpose of this study was to characterize the indentation deformation-fracture pattern in a selected single-crystal system, namely sapphire, using a transmission electron microscopy (TEM) procedure developed by Hockey.<sup>13</sup> The choice of sapphire was based principally on the requirement that the structure<sup>14,15</sup> and mechanical properties<sup>16</sup> should be reasonably well documented. (Another, longer-term motive was that the study should ultimately be extendable to practical ceramics, in this case to polycrystalline alumina, so that the influence of such microstructural variables as grain-boundary structure might be systematically evaluated.) Our principal goal was to identify the basic deformation elements associated with crack nucleation in sapphire, with the hope that this might allow us to make some statements about crystalline solids in general. Because crack nucleation is a critical first step in flaw development, we may anticipate our findings to be of relevance to important practical issues concerning the degradation of mechanical strength<sup>2</sup> (e.g., in small particle impact), wear and erosion, etc.

## II. Experimental Procedure

The method of specimen preparation for TEM examination was similar to that previously described by Hockey.<sup>13</sup> Disks (3-mm diameter) were cut using an ultrasonic drill from a thin slice of sapphire of  $(11\bar{2}0)$  orientation.\* This particular orientation was chosen because  $[11\bar{2}0]$  is the zone axis for a large number of planes that are susceptible to shear deformation (Section III). The disks were ground and polished to a thickness of 100 to 150  $\mu\text{m}$ . The final polishing step was carried out using 0.3- $\mu\text{m}$   $\text{Al}_2\text{O}_3$  powder to remove any remnant grinding damage which might be confused with the indentation structure. The samples were indented with a Vickers indenter at loads from 0.1 to 2.0 N, although for the majority of indentations a load of 0.25 N was used. The disks were then thinned by ion-beam milling from the back only, i.e. the side away from the indentation surface. Following carbon coating, the samples were examined in the TEM† at 150 keV. Some of the indented specimens were also examined by scanning electron microscopy (SEM) to reveal surface topographical features.

## III. Results

### (1) General Features

The indentation sites were readily identified in the TEM as localized regions of intense diffraction contrast. Figure 1, which shows sites for two different Vickers orientations relative to the specimen surface, is a typical example. The characteristic spreading of radial crack arms outward from the impression corners is clearly evident in these micrographs. The intense contrast within the indentation zone, together with the ubiquitous appearance of bend contours about the peripheries, is strongly indicative of a high-strain deformation process. Closer inspection of the indentation zones reveals crystalline shear elements which we identify as mechanical twins and slip faults. Microcracking associated with these shear elements is also identified. Details of such identifications are given in the following subsections.

### (2) Shear Deformation Elements

(A) *Twins—Morphology:* Selected-area-diffraction TEM was used to identify some of the shear elements as basal twins. Examples are indicated in Figs. 1 to 4. For the  $(11\bar{2}0)$  foil orientation, the twin planes are perpendicular to the plane of the foil and have surface traces perpendicular to the  $[0001]$ . No rhombohedral twins were detected. The same surface traces were visible in the

Received April 20, 1987; approved September 10, 1987.

Presented at the 89th Annual Meeting of the American Ceramic Society, Pittsburgh, PA, April 27, 1987 (Basic Science Division, Paper No. 35-B-87).

\*Supported by the U.S. Air Force Office of Scientific Research.

†Member, the American Ceramic Society.

\*Miller-Bravais indices corresponding to the structural unit cell  $c/a = 2.730$  are used throughout this paper.<sup>14</sup>

†Model EM 430, Philips Electronic Instruments, Inc., Mahwah, NJ.

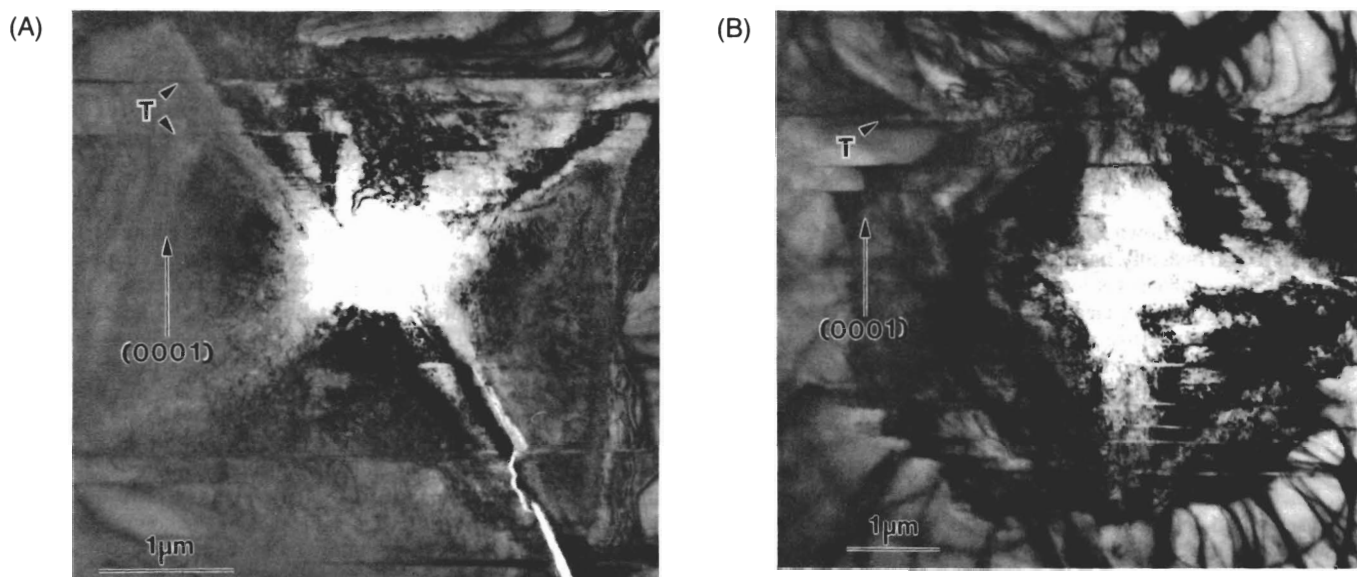


**Fig. 1.** TEM micrographs of 0.25-N Vickers indentations in sapphire: (A) Orientation A (indent diagonals at  $45^\circ$  to  $[0001]$ ). Basal twin ( $T$ ) density lower for the two quadrants where the impression edge is parallel to  $[0001]$ . (B) Orientation B (indent diagonals parallel and perpendicular to  $[0001]$ ). Basal twin density uniform in all four quadrants.



**Fig. 2.** SEM micrograph of 2-N Vickers indentation in sapphire, showing twin ( $T$ ) and slip ( $S$ ) traces at the surface. Radial cracks initiate from near impression corners.

SEM by topographical contrast (Fig. 2), indicating that the shear direction has a component normal to the foil (e.g.,  $[10\bar{1}0]$  or  $[01\bar{1}0]$  relative to the  $(11\bar{2}0)$  surface orientation). The morphological evidence is therefore consistent with a twinning plane ( $K_1$ ) =  $(0001)$  and twinning direction ( $\sigma_1$ ) =  $\langle 10\bar{1}0 \rangle$ . By viewing the shear planes edge-on, e.g., as in Fig. 3(A), the width of the twins was determined to be 10 to 50 nm.

The density of twins within the four quadrants of the indentation zone was found to depend on the orientation of the indenter. It can be seen that for orientation A in Fig. 1(A) the twins are located almost exclusively in the two quadrants whose impression edges lie perpendicular to  $[0001]$ . For orientation B in Fig. 1(B), on the other hand, the twin density is more or less equal in all four quadrants. This absence of twins in the left and right quadrants for orientation A may be rationalized in terms of the stress trajectory field beneath the indenter;<sup>1,7,9</sup> the basal planes in these two quadrants lie *normal* to the surfaces that experience the greatest punch-type shear stresses (see Fig. 9, later). In all other quadrants there is some component of resolved shear stress along the twinning direction. Herein lies our first strong manifestation of crystallographic constraint. It will be appreciated that the extreme anisotropy in twinning density means that there *must* exist other, perhaps more potent, shear deformation modes; for, otherwise, how might we possibly account for the residual impression in

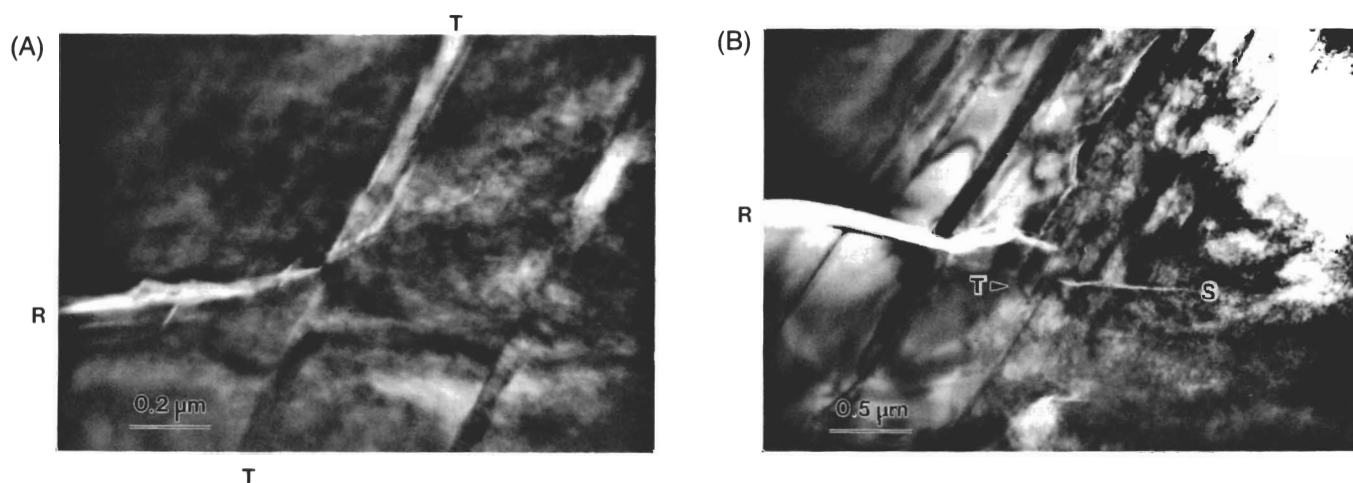


**Fig. 3.** Microcracks in indentation zone in sapphire (for orientation A, Fig. 1): (A) at basal twin interfaces near impression edge, showing nucleation along twin ( $TT$ ); (B) at intersections between twins ( $T$ ) and slip faults ( $S$ ) near impression corner. Note how microcracks evolve into radial arms at left.

twin-free quadrants such as those in Fig. 1?

These observations of the twin patterns were typical of all the indentation sites examined in this study; the only noteworthy departure from complete similarity was an apparent, slight tendency for the average thickness and the density of the twins to increase with load.

**(B) Slip Faults—Morphology and Misorientation:** Attempts were made to resolve the slip elements responsible for the bulk of the residual deformation in the central indentation zone. This proved difficult owing to the extremely high strain density. Nevertheless, by systematically tilting the foils in the TEM it was possible to image fault planes of localized high dislocation density, e.g., as seen in Figs. 3(B) and 4. These faults generally appeared to be much narrower than their twin counterparts and were interpreted as planes of concentrated slip. Selected-area diffraction in such regions showed no spurious reflections, confirming that the defects were *not* microtwins. From the TEM evidence, along with corresponding observations of fault traces in the SEM (e.g., Fig. 2), the slip plane for the faults was determined to be  $\{11\bar{2}3\}$ , i.e., of the pyramidal type. Because of the extreme intensity of contrast, attempts at Burgers vector determinations of the dislocations were unsuccessful.

Accordingly, another means was sought by which more quantitative information on the associated deformation might be obtained. Convergent-beam kikuchi patterns were used for this purpose. Thus the relative change in orientation in moving from the center to the edge of the indentation zone, in the manner shown schematically in Fig. 5(A), was mapped from the corresponding series of

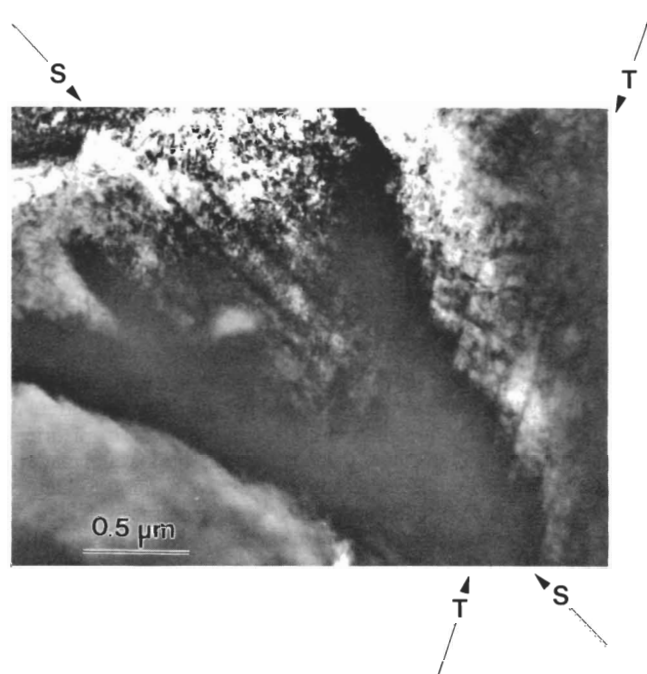


Fig. 4. TEM micrograph of 0.25-N Vickers indentation near impression corner in sapphire. Slip faults *SS* represent planes of concentrated slip lying parallel to  $\{11\bar{2}3\}$ . Twins *TT* also visible.

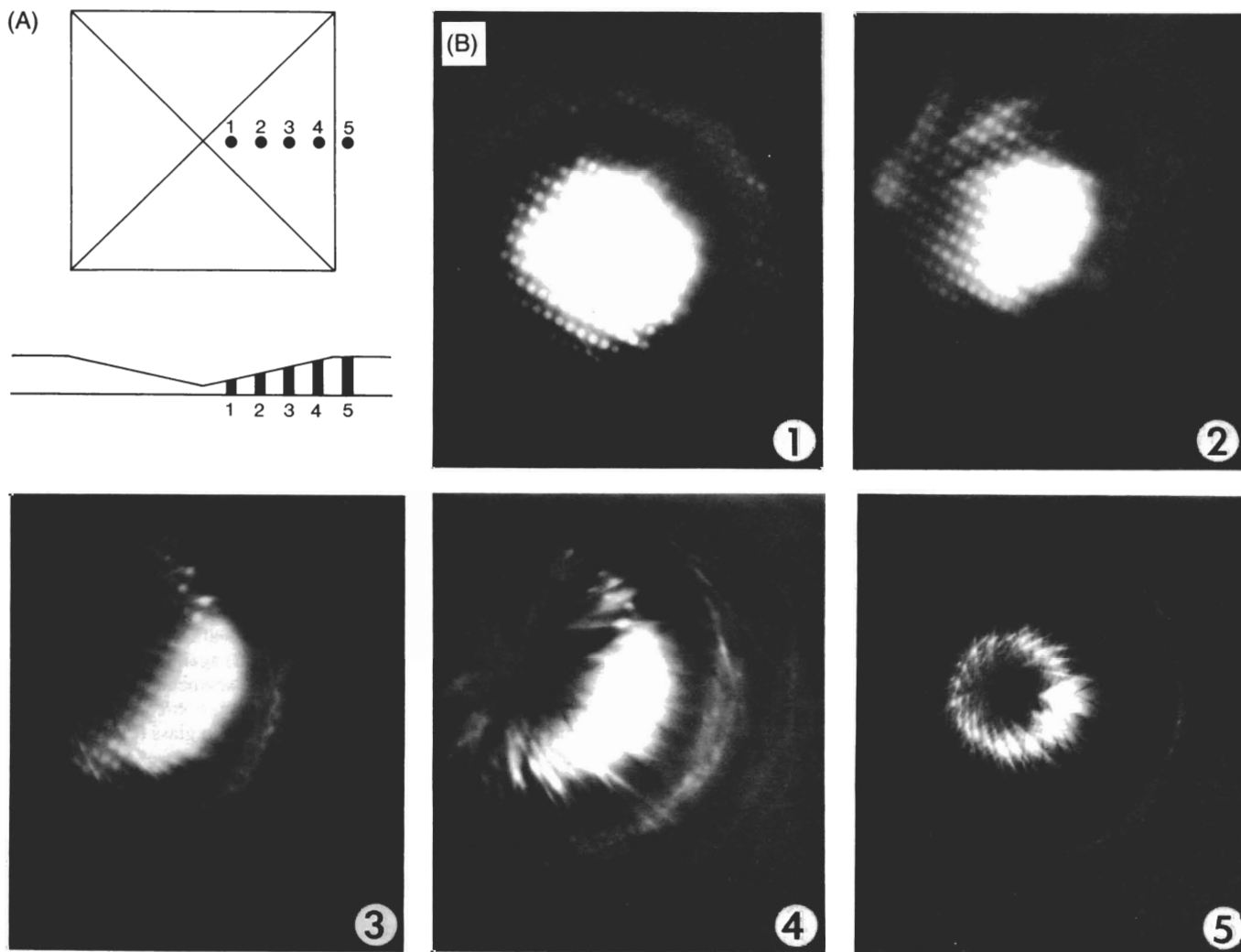


Fig. 5. Use of convergent-beam kikuchi patterns to measure misorientation within indentation zone: (A) Schematic, showing spot traverse for mapping out lattice rotations across each quadrant of indentation: upper diagram, plan view; lower diagram, profile view. (B) The corresponding kikuchi patterns.

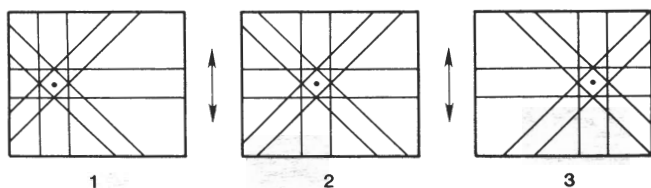


Fig. 6. Schematic diagram indicating invariant tilt axis (parallel to arrows) where the shift  $1 \rightarrow 2 \rightarrow 3$  in Kikuchi patterns is collinear.

Kikuchi patterns, Fig. 5(B). The electron probe size was  $\sim 0.1 \mu\text{m}$ , and typically five patterns were obtained per quadrant (including at least one outside the indentation area, to give a "zero misorientation" calibration). Because the position of the Kikuchi pattern relative to the transmitted spot is highly sensitive to minute changes in orientation, the shift between successive patterns provides us with an accurate measure of the misorientation. More specifically, the magnitude of the shift determines the angle of misorientation,  $\gamma$ , and the direction of the shift determines the axis of misorientation (Fig. 6). The values of  $\gamma$  in the near-center regions of the indentation (i.e., positions 1 to 4 in Fig. 5(A)) ranged from  $2^\circ$  to  $10^\circ$ ; this range appeared to be independent of load. These values are too high to be simply due to foil bending. Indeed,  $\gamma = 6^\circ$  corresponds to a shear strain  $\tan \gamma \approx 0.1$ , which is of the order of the theoretical cohesive limit.<sup>17</sup> This result is not surprising when one considers the ratio of hardness to shear modulus for sapphire,  $H/G \approx 20 \text{ GPa}/150 \text{ GPa} \approx 0.13$  (recalling that, by definition, hardness is a measure of the "average" stress beneath the indenter). It is clear that we are dealing with a high-stress shear process here.

The slip configurations were sensitive to the indent orientation. For orientation B the direction of the Kikuchi pattern shifts tended to be collinear, indicating that material rotation was taking place about an invariant tilt axis. This tilt axis was consistent with slip on a single crystallographic system (specifically, on  $\{11\bar{2}3\}\langle\bar{1}100\rangle$ ). For orientation A, however, although the magnitudes of the misorientations were similar, there was no such invariant tilt axis.

The difference in behavior between the two orientations can be explained by reference to Fig. 7. In this figure surface traces of the active  $\{11\bar{2}3\}$  planes (imaged in the TEM as planes of concentrated slip) are sketched in as dashed lines.\* Only two of the three possible surface traces are shown, as no evidence for slip was obtained for the third set. For orientation B one set of  $\{11\bar{2}3\}$  planes, that with its trace more closely parallel to the impression edge, is clearly more disposed to slip than the other. For orientation A symmetry prevails, so the two sets are equally well disposed to slip. Hence the lack of a well-defined tilt axis in the latter orientation.

As mentioned above, each trace actually represents a pair of planes; it is assumed, however, that only the plane which experiences the greater component of the shear stress<sup>7</sup> will be active. It is believed that although the third set of  $\{11\bar{2}3\}$  planes (surface trace perpendicular to the  $[0001]$ ) would appear to be favorably oriented for slip in orientation A, basal twinning occurs preferentially.

### (3) Microcracks

Particular attention was given to the presence of fine micro-

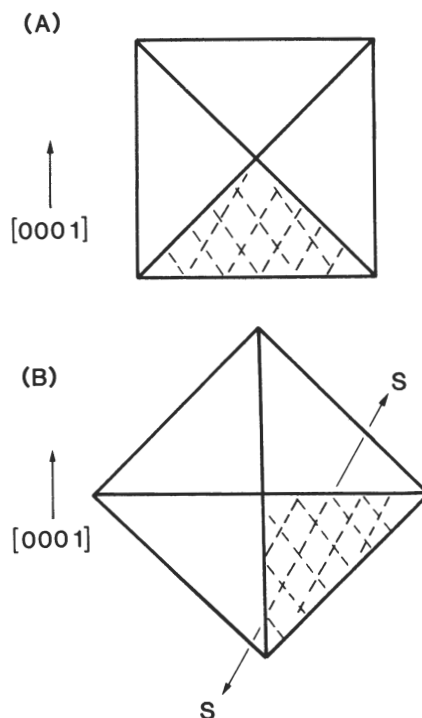


Fig. 7. Diagram showing trace of  $\{11\bar{2}3\}$  planes (shown as dashed lines) with respect to the indenter for orientations A and B. In orientation A the two sets of  $\{11\bar{2}3\}$  planes are symmetrically oriented with respect to the indenter. In orientation B preferred slip occurs on set of  $\{11\bar{2}3\}$  planes SS. Hence unique tilt axis in latter case.

cracks within the indentation zone, with the express intent of determining the source of nucleation centers for large-scale radial fracture. Examples are shown in Figs. 3, 4, and 8. No such microcracks were ever detected in the undisturbed crystal regions, eliminating the possibility that we might simply be observing a preexistent flaw population. Further, the incidence of microcracks appeared to be as great in the thicker regions of the foil as in the thinner, suggesting that the results are no mere artifacts of the foil preparation.<sup>8</sup>

By tilting the foil until the cracks were seen edge-on, it could be determined that nucleation occurred preferentially at either the  $\{11\bar{2}3\}$  slip planes or the  $(0001)$  twin interfaces. Figures 3 and 8 show examples. In Fig. 3(A) we see twin-induced microfissures along  $TT$  degenerating into a larger-scale radial crack  $R$  at lower left. (Close inspection reveals that the radial crack actually extends back a little way to the right, into the indentation zone.) It is noted that  $(0001)$  is not a favored cleavage plane in sapphire, so it is difficult to envisage how these fissures might ever be interpreted as anything other than the result of nucleation events. In Fig. 8 analogous, slip-plane fissures are evident, again degenerating into a radial crack configuration. We note the segmented appearance of this particular crack system near the impression corner, strikingly reminiscent of the radial patterns observed in glass (e.g., Fig. 7 in Ref. 9).

## IV. Discussion

Using electron microscopy, we have been able to identify basal twinning and pyramidal slip as the principal shear deformation elements for Vickers indentations in  $(11\bar{2}0)$  sapphire. In addition, we have observed microcracking associated with the shear elements. These processes all operate at stress levels close to the

\*It should be noted that altogether there are six variants of the  $\{11\bar{2}3\}$  plane. These can be regarded as consisting of three pairs of variants, where within each pair the two planes intersect the  $(11\bar{2}0)$  plane along the same direction, but are inclined at equal and opposite angles to the specimen surface.

<sup>8</sup>Note that even if foil relaxations were to be a factor, our conviction that we are witnessing intrinsic nucleation processes would hardly be diminished; such spurious relaxations might then be viewed as causing essentially the same (but premature) opening of the microcracks as would ultimately occur in any subsequent external loading.

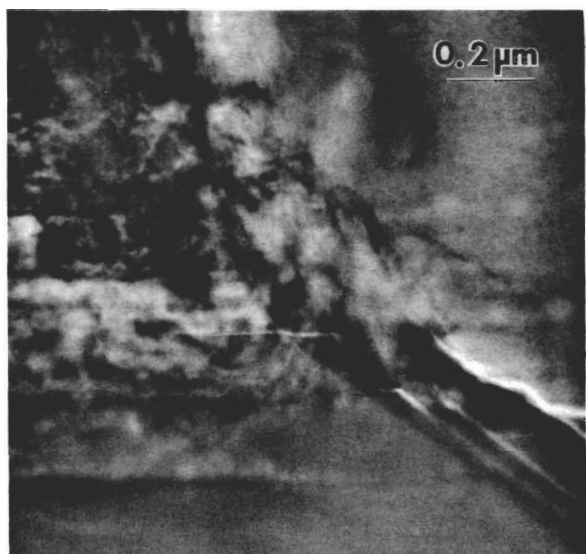


**Fig. 8.** TEM of 0.25-N Vickers indentation in sapphire, showing how slip faults intersect at impression corner to nucleate microcracks and thence to initiate the larger-scale radial cracks. Note crack "segments" parallel to impression diagonal in corner region. This suggests that, on sensing the tensile stress field that exists outside the hardness zone, the newly created microcracks make several unsuccessful attempts to "pop in" to the radial configuration, only to be arrested by an adjacent fault further removed from the center.

theoretical cohesive limit. In this respect the nature of the contact damage in sapphire appears to differ little from that in glassy materials. However, the anisotropy in deformation patterns for different indenter orientations (Fig. 1) indicates that crystallography imposes severe constraints on the capacity of the contact stress fields to activate slip. It is in this context that we discuss in some detail, with reference to Fig. 9, the manner in which the sapphire deforms to accommodate the penetrating indenter and thereby generates microcracks.

### (1) Deformation Mechanisms

Basal twinning has been observed in sapphire by several other workers.<sup>18-20</sup> What is perhaps surprising is that no evidence of *rhombohedral* twinning<sup>19,20</sup> was detected here. We have already alluded (Section III) to a strong crystallographic constraint factor in sapphire; it is therefore possible that the rhombohedral type could be activated in other foil and indenter orientations. It can thus be argued that we are dealing with highly competitive deformation processes in this material and that, for our {11 $\bar{2}$ 0} surface orientation, it is the basal plane, by virtue of its favorable disposition relative to the directions of principal shear, that is strongly favored.

Although basal twinning can accommodate *some* of the permanent deformation induced by the indenter, it cannot account for all of it. To see this, consider the twinning geometry in Fig. 9(A). It is readily shown that the semiangle of the hardness impression is given by

$$\tan \phi = [d/(d + D)] \tan \alpha \quad (1)$$

where  $D$  is the mean spacing between twins,  $d$  is the twin thickness, and  $\alpha$  is the twin shear angle. Inserting appropriate values,  $D \approx 500$  nm and  $d \approx 50$  nm from the electron microscopy evidence, and  $\alpha = 35^\circ$  from geometrical considerations, we calculate  $\phi \approx 4^\circ$  for the impression angle. This is substantially less than the corresponding angle  $16^\circ$  between the faces of the Vickers pyramid and the specimen surface. It is clear that other deformation mech-

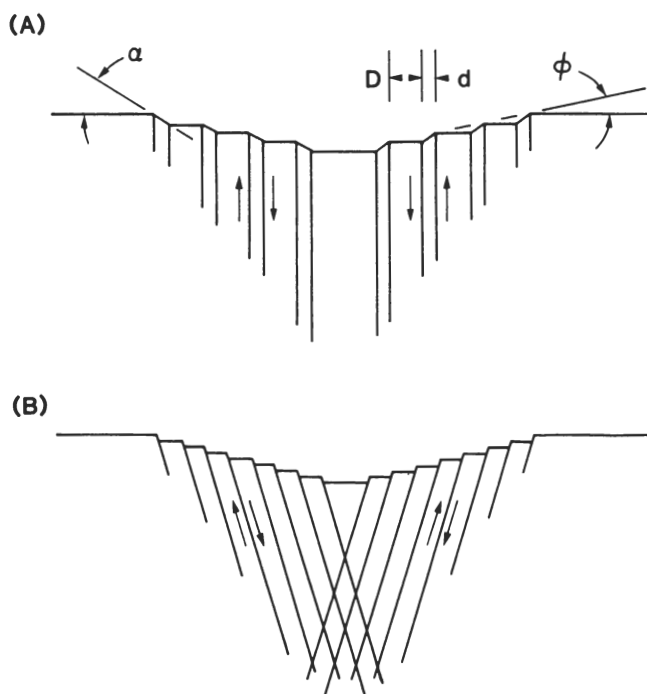


**Fig. 9.** Schematic illustration of how (A) twinning and (B) slip act to accommodate the punch-type shear stresses induced by the indenter.

anisms must act in concert with the twinning.

Our results indicate that pyramidal slip, Fig. 9B, is predominant among these other deformation modes. This is in accord with previous sharp particle impact work by Hockey<sup>18</sup> on {11 $\bar{2}$ 3} surfaces; for that particular contact configuration it was possible to resolve individual dislocation arrays at the periphery of the deformation zone, and thence to confirm the {11 $\bar{2}$ 3}<1100> primary system. However, the detailed nature of the slip process remains somewhat obscure, particularly in the regions of highest stress concentration (i.e., at the impression center and diagonals). We have mentioned the difficulties in carrying out Burgers vector determinations in the regions of intense diffraction contrast. Given the strong inhomogeneity of the typical indentation stress field,<sup>1</sup> together with the constraints imposed by the indenter shape (especially at the contact diagonals), it is not unreasonable to expect that some multiple slip-plane activity must occur.

The fact that the slip processes operate close to the cohesive limit means that there are high Peierls energy barriers to dislocation motion. High Peierls barriers are, of course, characteristic of all ceramics as a large component of covalent bonding.<sup>17</sup> The question arises as to how valid it is to retain the picture of plasticity by (activated) glide dislocation motion in such cases. Hill and Rowcliffe,<sup>22</sup> in analyzing analogous indentation-induced dislocation structures in silicon, suggested a catastrophic shear mechanism, for which they coined the term "block slip." In their interpretation the observed dislocations simply represent the end result of lattice mismatch between opposing, slipped surfaces, somewhat akin to the configuration one would expect for a healed shear crack. It might be argued that such distinctions amount to no more than an exercise in semantics; after all, the final dislocation array is the same. On the other hand, the concept of block slip, unlike that of simple dislocation motion, does extend naturally to noncrystalline materials; thus the shear faulting observed in glass<sup>7-10</sup> may well be described in these terms.

### (2) Crack Nucleation

Regardless of the detailed nature of the shearing process in sapphire, it is apparent that the slip planes, as well as the twin



interfaces, can be viewed as high-energy planar defects. As such, they represent favored sites for microcrack nucleation, consistent with the experimental results in Section III. We are unaware of any study of crack nucleation in sapphire in the literature (apart from inferences drawn from incidental observations, e.g., postfailure fractography of strength specimens<sup>23</sup>), so we shall explore the possible mechanism in greater detail below.

First, it may be reiterated that we are dealing with true nucleation events here, and not simply with the propagation (if stable) of preexisting flaws. Experimental studies on double-cantilever beam fracture specimens<sup>24</sup> demonstrate that (0001) is the *least* favored of all crystallographic planes for cleavage (a result that is readily rationalized in terms of the high cost in energy to separate surfaces of oppositely charged ions). Yet one of the sets of microcracks in our indentation experiments was observed at the basal twin interfaces. Such energetically unfavorable fracture configurations are to be expected only under conditions of extraordinary constraint, as indeed occur beneath a Vickers indenter. There the local stress concentrations are presumably so intense, with a strongly suppressed tensile component, as to override the usual dominating influence of surface energy.<sup>1</sup>

Accordingly, by analogy with the shear-fault modeling in earlier studies on glass,<sup>9,26</sup> it is proposed that crack nucleation in sapphire occurs preferentially on the twin and slip interfaces. Exactly where along these interfaces the nucleation begins is open to speculation, but there are certain sites that appear more favored than others. Among these are points of intersection between twin and slip planes in adjacent quadrants, especially in the vicinity of the impression diagonals.<sup>9</sup> There are strong parallels here with the time-honored dislocation pileup models of crack initiation of the Zener-Stroh-Cottrell type<sup>27-29</sup> for metals. An important difference in the covalent-ionic material of interest here is that the "pileup" planes themselves, because of their state of high energy, are likely to become an integral part of the crack embryos once the process has begun. It follows that for "subthreshold" indentations in which nucleation has not yet been effected, these planes will remain as potential sources of weakness in any subsequent, external stressing and/or environmental attack, as is indeed found to be the case in optical glass fibers.<sup>30</sup>

The issues raised above have important implications concerning the mechanical properties of intrinsically hard, brittle ceramics. It is generally accepted that the chief cause of strength degradation in ceramic materials with initially pristine surfaces is the presence of small "flaws," and yet scant attention has been paid to the fundamental, precursor defects from which these flaws generate. Instead, there is a deeply rooted tendency for those involved in strength analysis to disregard such potential "complications," and to treat flaws as scaled-down versions of large-scale cracks subject exclusively to externally applied stresses. The results of our study indicate that this picture can be highly oversimplistic. Not only may the response of these flaws in external fields be dominated by the residual nucleation stresses and local crystallographic constraints, but the flaws themselves may exist in a "subthreshold" state. In such cases the mechanics of failure differ dramatically from those that derive from the traditional "Griffith microcrack" theories.<sup>31</sup> We may envisage a similar impact on the micro-mechanics of other, practically important, contact-related processes, such as erosion by particle impact, and wear by machining, grinding, and polishing, etc. The additional complications that will inevitably occur in *polycrystalline* aluminas and other engineering ceramics remain a subject for future investigation.

## V. Conclusions

For the indentation of {1120} sapphire, the deformation processes which occur have been shown to be sensitive to the orientation of the indenter with respect to the crystallography. The principal modes of deformation were identified as basal twinning, and pyramidal slip. The basal twin interfaces and pyramidal slip planes were observed to act as nucleation sites for incipient microcracks. Since these interfaces represent planes of weakness in the structure, one can consider flaws as existing along these boundaries in a subthreshold state. The findings of our studies on crack nucleation processes suggest that the concept of a "Griffith microcrack," which is subject (in its mechanical response) only to external stress fields, may be overly simplistic.

**Acknowledgments:** The authors thank B. J. Hockey for help and advice on the preparation of specimens for the TEM, and for many long and stimulating discussions on the nature of the twin and slip plane processes; A. J. Shapiro for help with the SEM work; and S. M. Wiederhorn for comments on the indentation damage.

## References

- <sup>1</sup>B. R. Lawn and T. R. Wilshaw, "Indentation Fracture: Principles and Applications," *J. Mater. Sci.*, **10** [6] 1049-81 (1975).
- <sup>2</sup>B. R. Lawn; pp. 1-25 in *Fracture Mechanics of Ceramics*, Vol. 5. Edited by R. C. Bradt, D. P. H. Hasselman, and F. F. Lange. Plenum Press, New York, 1983.
- <sup>3</sup>B. R. Lawn; pp. 67-86 in *Strength of Glass*. Edited by C. R. Kurkjian. Plenum Press, New York, 1985.
- <sup>4</sup>A. G. Evans and E. A. Charles, "Fracture Toughness Determinations by Indentation," *J. Am. Ceram. Soc.*, **59** [7-8] 371-72 (1976).
- <sup>5</sup>G. R. Anstis, P. Chantikul, D. B. Marshall, and B. R. Lawn, "A Critical Evaluation of Indentation Techniques for Measuring Fracture Toughness: I, Direct Crack Measurements," *J. Am. Ceram. Soc.*, **64** [9] 533-39 (1981).
- <sup>6</sup>P. Chantikul, G. R. Anstis, B. R. Lawn, and D. B. Marshall, "A Critical Evaluation of Indentation Techniques for Measuring Fracture Toughness: II, Strength Method," *J. Am. Ceram. Soc.*, **64** [9] 539-43 (1981).
- <sup>7</sup>J. T. Hagan and M. V. Swain, "The Origin of Median and Lateral Cracks at Plastic Indents in Brittle Materials," *J. Phys. D.*, **11** [15] 2091-102 (1978).
- <sup>8</sup>J. T. Hagan, "Shear Deformation Under Pyramidal Indenters in Soda-Lime Glass," *J. Mater. Sci.*, **15** [6] 1417-24 (1980).
- <sup>9</sup>B. R. Lawn, T. P. Dabbs, and C. J. Fairbanks, "Kinetics of Shear-Activated Indentation Crack Initiation in Soda-Lime Glass," *J. Mater. Sci.*, **18** [9] 2785-97 (1983).
- <sup>10</sup>H. Mulhopp, B. R. Lawn, and T. P. Dabbs; pp. 681-93 in *Deformation of Ceramic Materials*, II. Edited by R. C. Bradt and R. E. Tressler. Plenum Press, New York, 1984.
- <sup>11</sup>D. B. Marshall and B. R. Lawn, "Residual Stress Effects in Sharp-Contact Cracking: I," *J. Mater. Sci.*, **14** [8] 2001-12 (1979).
- <sup>12</sup>D. B. Marshall, B. R. Lawn, and P. Chantikul, *J. Mater. Sci.*, **14** [9] 2225-35 (1979).
- <sup>13</sup>B. J. Hockey, "Plastic Deformation of Aluminum Oxide by Indentation and Abrasion," *J. Am. Ceram. Soc.*, **54** [5] 223-31 (1971).
- <sup>14</sup>M. L. Kronberg, "Plastic Deformation of Single Crystals of Sapphire," *J. Am. Ceram. Soc.*, **5** [9] 507-24 (1975).
- <sup>15</sup>A. H. Heuer and J. Castaing; pp. 238-57 in *Advances in Ceramics*, Vol. 10. Edited by W. D. Kingery. American Ceramic Society, Columbus, OH, 1984.
- <sup>16</sup>R. M. Cannon; pp. 818-38 in *Advances in Ceramics*, Vol. 10. Edited by W. D. Kingery. American Ceramic Society, Columbus, OH, 1984.
- <sup>17</sup>A. Kelly, *Strong Solids*; pp. 1-35. Clarendon Press, Oxford, 1966.
- <sup>18</sup>B. J. Hockey, "Pyramidal Slip and Basal Twinning in Aluminum Oxide"; pp. 167-79 in *Deformation of Ceramic Materials*, I. Edited by R. C. Bradt and R. E. Tressler. Plenum Press, New York, 1975.
- <sup>19</sup>A. H. Heuer, "Deformation Twinning in Corundum," *Philos. Mag. A*, **13** [122] 379-93 (1966).
- <sup>20</sup>E. Stofel and H. Conrad, "Fracture and Twinning in Sapphire ( $\alpha$ -Al<sub>2</sub>O<sub>3</sub>) Crystals," *Trans. Metall. Soc. AIME*, **227** [5] 1053-60 (1963).
- <sup>21</sup>W. D. Scott; pp. 235-49 in *Deformation of Ceramic Materials*, II. Edited by R. C. Bradt and R. E. Tressler. Plenum Press, New York, 1984.
- <sup>22</sup>M. J. Hill and D. J. Rowcliffe, "Deformation of Silicon at Low Temperatures," *J. Mater. Sci.*, **9** [10] 1569-76 (1974).
- <sup>23</sup>P. F. Becher, "Fracture-Strength Anisotropy of Sapphire," *J. Am. Ceram. Soc.*, **59** [1-2] 59-61 (1976).
- <sup>24</sup>S. M. Wiederhorn, "Fracture of Sapphire," *J. Am. Ceram. Soc.*, **52** [9] 485-91 (1969).

<sup>5</sup>It is interesting to note that sapphire is not the only material in which indentation-induced cracking on other than primary cleavage planes is observed. In both LiF and MgO, radial crack arms can be made to extend relatively large distances along {110} planes, even though it is {001} which constitute the easy fracture planes;<sup>25</sup> there, because of the relative softness of the material, the critical slip events responsible for the generation of the noncleavage cracks are much more readily apparent.

<sup>25</sup>B. R. Lawn and D. B. Marshall, "Indentation Fractography: A Measure of Brittleness," *J. Res. Natl. Bur. Stand (U.S.)*, **89** [6] 435–51 (1984).

<sup>26</sup>J. T. Hagan, "Micromechanics of Crack Nucleation During Indentations," *J. Mater. Sci.*, **14** [12] 2975–80 (1979).

<sup>27</sup>C. Zener, pp. 3–31 in *Fracturing of Metals*. American Society of Metals, Cleveland, OH, 1948.

<sup>28</sup>A. N. Stroh, "The Formation of Cracks as a Result of Plastic Flow," *Proc. R. Soc. London, Ser. A*, **A223**, 404–14 (1954).

<sup>29</sup>A. H. Cottrell, "Theory of Brittle Fracture in Steels and Similar Metals," *Trans. Metall. Soc. AIME*, **212** [2] 192–203 (1958).

<sup>30</sup>T. P. Dabbs and B. R. Lawn, "Strength and Fatigue Properties of Optical Glass Fibers Containing Microindentation Flaws," *J. Am. Ceram. Soc.*, **68** [11] 563–69 (1985).

<sup>31</sup>E. R. Fuller, B. R. Lawn, and R. F. Cook, "Theory of Fatigue for Brittle Flaws Originating from Residual Stress Concentrations," *J. Am. Ceram. Soc.*, **66** [5] 314–21 (1983). □